Postprint of: Kumar S., Kilich T., Łabuda M., García G., Limão-Vieira P., Anionic states of C_6C_{l6} probed in electron transfer experiments, PHYSICAL CHEMISTRY CHEMICAL PHYSICS Vol. 24, No 1 (2021), pp. 366-374, DOI: 10.1039/D1CP04500H

Anionic states of C_6Cl_6 probed in electron transfer experiments

S. Kumar[1], T. Kilich[2], M. Łabuda[2], G. García[3], and P. Limão-Vieira[1,*]

[1] Atomic and Molecular Collisions Laboratory, CEFITEC, Department of Physics, Universidade NOVA de Lisboa, 2829-516 Caparica, Portugal

[2] Department of Theoretical Physics and Quantum Information, Gdańsk University of Technology, Narutowicza 11/12, 80-233 Gdańsk, Poland

[3] Instituto de Física Fundamental, Consejo Superior de Investigaciones Científicas (CSIC), Serrano 113-bis, 28006 Madrid, Spain

ABSTRACT

This is the first comprehensive investigation on the anionic species formed in collisions of fast neutral potassium (K) atoms with neutral hexachlorobenzene (C_6Cl_6) molecules in the laboratory frame range from 10 up to 100 eV. In such ion-pair formation experiments we also report a novel K^+ energy loss spectrum obtained in the forward scattering giving evidence of the most accessible electronic states. The vertical electron affinity of (–3.76 ± 0.20) eV has been obtained and assigned to a purely repulsive transition from C_6Cl_6 ground state to a σ_{CCl}*state of the temporary negative ion yielding Cl^- formation. These experimental findings have also been supported by state-of-the art theoretical calculations on the electronic structure of C_6Cl_6 in the presence of a potassium atom and used to help analyse the lowest unoccupied molecular orbitals participating in the collision process. From the time-of-flight mass spectra recorded in the wide collision energy range, more than 80% of the total anion yield is due to the undissociated parent anion $C_6Cl_6^-$, $C_6Cl_5^-$ and Cl^- formation. Other fragment anions that require complex internal reactions within the temporary negative ion formed after electron transfer, and accounting for less than 20% of the total yield, have been assigned to $C_6Cl_4^-$, $C_3Cl_2^-$, C_2Cl^- and Cl_2^-. The joint experimental and theoretical methodologies employed in these electron transfer studies, are the most comprehensive and unique assignments of the hexachlorobenzene anionic species and the role of C_6Cl_6 electronic states in collision induced dissociation to date.

* E-mail: plimaovieira@fct.unl.pt; Fax: +351 212948549; Tel: +351 212947859

1 Introduction

Hexachlorobenzene (C_6Cl_6), as part of a large group of volatile organochloride compounds, has been used as a pesticide across the globe,[1,2] and found to be a prevailing environmental pollutant.[3] Its global distribution revealed it moves through the atmosphere from warmer source regions (where it is volatilized) and tend to condense at colder regions,[4–6] undergoing a process known as global distillation.[1,4] In the atmosphere, reactions with $^{\bullet}OH$ radicals have been identified as a sink mechanism,[1] yet the relative low rate constant, 0.27×10^{-13} cm^3 molecules^{-1} s^{-1} at 298K, favours such global distillation process.[1] C_6Cl_6 can be eliminated by ozone coupled with hydrogen peroxide processes and these can be enhanced by combination with active carbon absorption methods.[2,7] Additionally, the lack of comprehensive photolysis rates in the literature do not allow identifying ultra-violet photoabsorption as a route to remove and/or chemically change these molecular compounds in the Earth's atmosphere.

Hexachlorobenzene has been investigated by experimental and theoretical methods, the former dealing with ultraviolet photoabsorption,[8,9] infrared photoabsorption[10,11], photoelectron spectroscopy,[12] gas-phase reactions with molecular oxygen[13] and reduction potentials with an electron capture detector (ECD)[14]; the latter on vibronic interactions and charge transfer[15] and electron affinities of chlorinated benzene molecules.[16–18] Photodegradation of C_6Cl_6 and theoretical prediction of its pathways using quantum chemical calculation has been reported by Yamada et al.[19] As far as negative ion formation is concerned, a comprehensive literature survey reveals only the parent anion from resonance electron capture mass spectrometry, allowing to determine an adiabatic electron affinity of 0.91 eV,[13] whereas a value of 0.98 eV has been reported by Wiley and co-workers.[17] Moreover, the generalized Kohn-Sham semicanonical projected random phase approximation method, predicts a valence π* character for $C_6Cl_6^-$ ground-state,[16] while Robin[9] has noted that the most relevant absorption features at 42500 cm^{-1} ($^1A_{1g} \rightarrow {}^1B_{1u}$) and 46000 cm^{-1} ($^1A_{1g} \rightarrow {}^1E_{1u}$) in neutral C_6Cl_6 have been assigned to intense halogen np → π* charge transfer transitions.

The molecular orbitals configuration of C_6Cl_6 in D_{6h} symmetry yields for the outer valence … $(e_{1g})^4$ corresponding to the $^1A_{1g}$ sate, while the parent anion results from electron capture into the non-degenerate a_{1g} lowest unoccupied molecular orbital with configuration … $(e_{1g})^4\,(a_{1g})^1$ which corresponds to $^2A_{1g}$ state, with no appreciable Jahn-Teller effect.[15] Given the lack of any other relevant information on negative ion formation from hexachlorobenzene either by dissociative electron attachment or charge transfer processes, a comprehensive investigation of the underlying molecular mechanisms yielding $C_6Cl_6^-$ and its fragment anions

is necessary for getting further knowledge on the electronic structure of such chemical compound.

In this study, we present for the first time a comprehensive investigation of hexachlorobenzene negative ions formation in electron transfer processes, combining experimental and state-of-the art theoretical methods. In Sec. 2, we present a brief summary of the experimental setup and in Sec. 3 the computational details of the calculations used to help the interpretation of experimental data. Section 4 is dedicated to results and discussion, which includes a complete description of the electronic state spectroscopy of hexachlorobenzene probed by the experimental method and supported by quantum chemical calculations. The data have been used to assign the nature of the lowest-lying electronic states accessed in electron transfer processes in neutral potassium collisions with neutral hexachlorobenzene molecules. We finish with Sec. 5 by including a summary and conclusions.

2 Experimental methods

The crossed molecular beam setup used to investigate negative ion formation in collisions of neutral potassium (K) atoms with hexachlorobenzene (C_6Cl_6) molecules was previously described elsewhere,[20] therefore only a general description is given here. Briefly, an effusive target molecular beam crosses a projectile beam of neutral hyperthermal K atoms and the product anions formed in the electron transfer process are analysed by a dual-stage linear time-of-flight (TOF) mass spectrometer. The K beam is produced in a charge exchange chamber from the interaction of gas-phase neutral potassium atoms from an oven source with accelerated K^+ ions emitted from a commercial ion source (HeatWave, US) in the range of 10 to 100 eV in the lab frame. The intensity of the neutral potassium beam is monitored using a Langmuir-Taylor ionisation detector, before and after collecting the mass spectra. The TOF anion yield is normalized considering the primary beam current, pressure and acquisition time. The typical base pressure in the collision chamber was 4×10^{-5} Pa and the working pressure was 1×10^{-3} Pa. Mass calibration was performed on the basis of the well-known anionic species formed after potassium collisions with nitromethane[20] and tetrachloromethane.[21]

A hemispherical energy loss analyser was used to obtain the K^+ signal post-collision in the forward scattering direction with the beam's optical path, where such experiments were not performed in coincidence with TOF mass spectrometry. The analyser was operated in constant transmission mode, hence keeping the resolution constant throughout the entire scans. The estimated energy resolution during the experiments was ~1.2 ± 0.2 eV. The energy loss scale was calibrated using the K^+ beam profile from the potassium ion source serving as the *elastic*

peak. Hexachlorobenzene (C_6Cl_6) was supplied by Sigma Aldrich with a stated purity of ≥ 98%. The solid sample was used as delivered and gently heated up to to 340 K through a temperature PID (proportional-integral-derivate controller) unit. In order to test for any thermal decomposition products within the hexachlorobenzene beam, mass spectra were recorded at different temperatures and no differences in the relative peak intensities as a function of temperature were observed.

3 Theoretical methods

Charge transfer processes are described with the aid of *ab initio* calculations, based on the evolution of the quasi-molecular system, formed by the potassium projectile and the molecular target along the reaction coordinate within the framework of the molecular representation. This methodology has been successfully used for diatomic systems and tested in ion-neutral molecule collisions,[22–26] later extended to atom-molecule interactions[21,27,28] where the system evolves along the reaction coordinate corresponding to the distance R between the impact atom and the molecular target.[29–32] In such approximation, we do not include the internal degrees of freedom of the molecular target explicity, which is reasonable since collisional processes are very fast and thus nuclear vibrational and rotational motions are much slower than the collision time and can be considered frozen during the collision.

The geometry of hexachlorobenzene at D_{2h} symmetry was optimized at the MP2/def2-TVZP level of theory[33] while in the presence of potassium atom the C_{2v} symmetry was used. All calculations have been performed by means of the ORCA and MOLPRO packages of *ab initio* programmes.[34,35] The potassium atom has been placed along the y axis as shown in Fig. 1 and the C_6Cl_6 target is kept frozen in its ground state ($\tilde{X}$: $^1A'$) geometry during the collision process. A detailed analysis of the K-C_6Cl_6 interaction at R = [2.5, 5, 7.5, 10] Å, occurring between molecular states involved in this process, has been made in order to precisely determine asymptotic molecular configurations of the calculated states. The calculation has been carried out in Cartesian coordinates, with no symmetries. All electrons of carbon and chlorine atoms have been included in the calculations and their 1s orbitals were treated as frozen-core. For the potassium atom, the ECP18SDF core-electron pseudopotential[36] with the associated basis set has been chosen. The natural molecular orbitals for K–C_6Cl_6 (see supplementary information Fig. S1 and Table S1) have been obtained at state-averaged Complete Active Space Self Consistent Field (CASSCF)[37–39] level of theory considering the static electron correlation for the reaction coordinate K–C_6Cl_6 at R = 5 Å distance, corresponding to the asymptotic region. The resultant highest occupied (HOMOs) and the

lowest unoccupied molecular orbitals (LUMOs) for K–C_6Cl_6 are shown in Fig. 2 and Fig. S1 together with the corresponding orbitals without the presence of the potassium atom (see Fig. S2 and Table S2). Finally, Fig. S3 depicts $C_6Cl_6^-$ highest doubly occupied, singly occupied (SOMO) as well as the lowest unoccupied molecular orbitals (RKS, B3LYP+D3).

In order to determine the ionisation energy, electron affinity and vertical detachment energy (see Table S3) and to look closely at the anion where the symmetry is broken, DFT calculations have been performed where Kohn-Sham orbitals were used rather than canonical HF orbitals, since the former improve the agreement with the experimental electron affinity of C_6Cl_6 by 0.08 eV. In order to describe an extra electron, diffuse functions with additional augmented basis functions were used at the restricted open shell Kohn-Sham, B3LYP+D3 level of theory.[40] Energies of the neutral, the anion and the cation are -2989.57786, -2989.61393 and -2989.25288 hartree, respectively and resign from Table S4 in supplementary information.

4 Results and discussion

TOF mass spectra have been recorded in a wide range of lab-frame collision energies from 10 up to 100 eV (7.9 to 79.1 eV in the centre-of-mass frame), yielding negative ions assigned to Cl^-, Cl_2^-, C_2Cl^-, $C_3Cl_2^-$, $C_6Cl_4^-$, $C_6Cl_5^-$ and $C_6Cl_6^-$ along with their respective isotopes. Fig. 3 shows a typical mass spectrum recorded at 100 eV (E_{CM} = 79.1 eV), where the inset depicts the parent anion signal fitted with Gaussian functions to reproduce its isotope contributions at 282 u (51%), 284 u (100%), 286 u (81%) and 288 u (35%). Note that a TOF mass peak shows an apparent asymmetry relative to its maximum position, with typically the left-hand branch much steeper that the right-hand.[41] Yet, for the sake of example, the Gaussian fitting used reproduces quite well in magnitude and in shape the TOF mass signal. Another relevant aspect pertains to the Cl_2^- TOF mass contribution, where the peak should show its isotope contributions at 70 u (100%), 72 u (~65%), 74 u (~11%). A close inspection of this anion feature in Fig. 3 reveals that the peak contains three contributions but not in the expected intensity. Given the limited TOF mass resolution ($m/\Delta m \approx 125$) that does not allow to clearly resolve close fragment anions, yet a proper peak fitting, as that used for $C_6Cl_6^-$, reproduces perfectly well the expected isotope distribution intensities (see Fig. S4 in SI).

The energy loss spectrum of the potassium cations formed in the forward direction ($\theta \cong 0°$) of K atoms in collisions with C_6Cl_6 at 205 eV lab frame energy (E_{CM} = 162 eV), is shown in Fig. 4. Hexachlorobenzene branching ratios (fragment anion yield/total anion yield) of the main negative ions formed as a function of the collision energy in the centre-of-mass frame are depicted in Fig. 5.

From a close inspection of Fig. 3 TOF mass spectrum, the prevalent anion is assigned to Cl^-, followed by the undissociated parent anion and Cl_2^-, while other fragment ions are considerably less intense, *viz*. those resulting from the loss of Cl units and ring breaking. We have performed additional calculations on $C_6Cl_6^-$ to obtain the energy values of the orbitals with the restricted open shell Kohn-Sham B3LYP+D3 level of theory (see Fig. S3), where the electron spin densities show a preferential C–Cl bond excision yielding the chlorine anion (see discussion below). The calculated lowest unoccupied molecular orbitals in Fig. 2 show that the LUMO+4 and LUMO+5 σ* states are slightly shifted to lower energies (0.8–1.0 eV) in comparison to respective calculated MOs without the presence of the potassium atom.

4.1 K^+ energy loss data

The energy loss spectrum of K^+ ions formed in collisions of potassium atoms with hexachlorobenzene, has been obtained at 162.2 eV in the centre-of-mass frame (205 eV lab frame) in the forward direction ($\theta \cong 0°$) and is depicted in Fig. 4. We observe for the first time some low-intensity features and a main peak with maximum intensity (I_{max}) at (8.1 ± 0.2) eV. Electron transfer processes triggered by the collision of neutral potassium atoms (K) with neutral target molecules and yielding ion-pair formation, the energy loss required to access an electronic state, $\Delta E = IE(K) - EA(I_{max})$, with the difference between the potassium atom ionisation energy and the target molecule's electron affinity for that state,[42] which results on a vertical electron affinity of (–3.76 ± 0.20) eV. Gaussian fittings have been used to decompose the energy loss spectrum main peak, indicating the presence of adjacent contributions, as well as other low-intensity less resolved features with their vertical electron affinities listed in Table 1. Note that Voora[16] has assigned the lowest-lying character of $C_6Cl_6^-$ to a valence-bound (vb) π* state with an electron affinity EA (C_6Cl_6) varying from 0.03 up to 0.30 eV, depending on the basis set used, and an associated error of 0.13 eV.

4.2 $C_6Cl_6^-$ formation

The TOF mass spectra recorded in the wide collision energy range show that the undissociated parent anion accounts for more than 70% of the total ion yield for $E_{CM} < 10$ eV, whereas above 50 eV its BR is ~ 20% (Fig. 5). These results indicate that electron transfer is very efficiently captured by hexachlorobenzene and the process may proceed according to the reaction:

$$K + C_6Cl_6 \rightarrow (K^+\ C_6Cl_6^-) \rightarrow K^+ + (C_6Cl_6^-)^{\#} \rightarrow K^+ + C_6Cl_6^- \qquad (1)$$

with $(C_6Cl_6^-)^\#$ formation of a temporary negative ion (TNI) with an excess of internal energy.

Attachment of an electron is accompanied by significant energy release comprising the kinetic energy of the incoming electron and the molecule's electron affinity, which was calculated to be –0.14 eV (vertical) and 0.98 eV (adiabatic) at the RKS/B3LYP+D3/aug-cc-pVTZ level of theory (Table S3), the latter in good agreement with 0.91 eV and 0.98 eV from Knighton et al.[13] and Wiley et al.,[17] respectively. Since the collision energy is always above the threshold of ion-pair formation, the excess energy of the TNI (metastable) can lead to statistical and/or direct dissociation.[41] Formation of metastable parent anions and their detection within the TOF mass window (< 80 μs), has been observed in electron transfer experiments to cyclic and non-cyclic molecular compounds. The former may enable an efficient redistribution of the excess energy through the different internal degrees of freedom, e.g. nitroimidazoles,[43,44] the latter can be rationalised in terms of an efficient door-way for enhanced bond breaking such as nitromethane.[20] Hexachlorobenzene is a highly symmetric molecule with 30 vibrational degrees of freedom, thus providing an effective mean for energy redistribution, enhancing $C_6Cl_6^-$ yield in the low-energy collision range. As the collision energy is further increased, the parent anion yield decreases, meaning that in such energy range more energy is transferred to the target molecule enhancing fragmentation.

In the energy loss data of Fig. 4, the weak feature peaking at (3.1 ± 0.3) eV, yields a positive electron affinity of (1.24 ± 0.3) eV. Note that the asymptotic limit of $C_6Cl_5 + Cl^-$ is 0.56 eV, i.e. 0.35 eV below the ground state of the neutral[15,19] (C_6Cl_6) meaning that the feature at 1.24 eV does not lead to bond breaking resulting in $C_6Cl_6^-$ formation. There is no available information in the literature on the precise energy value of C–Cl stretching mode of the parent anion (372 cm^{-1} for the neutral ground state[12]), thus the lower limit of the electron affinity (0.94 eV) is in very good agreement with the adiabatic values reported by Knighton et al.[13] and Wiley et al.,[17] 0.91 and 0.98 eV, respectively, as well as the calculated value at the RKS/B3LYP+D3/aug-cc-pVTZ level of theory (see Tables 1 and S3).

4.3 $C_6Cl_5^-$ and Cl^- formation

The TOF mass spectra in Fig. 3 is dominated by Cl^- formation in the collision energy range above 10 eV, amounting to ~ 70% of the total anion yield above 40 eV (see BRs in Fig. 5). The dominance of such anion formation does not seem unexpected given the considerable high electron affinity of Cl (3.6131 eV[45]). Moreover, in the energy range above 40 eV, the Cl^- branching ratio shows a rather constant behaviour which is reminiscent of the fast collision

dynamics (collision time < 37 fs) dictated by direct vertical access within the Franck-Condon region to the ionic states. Hence, those prominent strong antibonding character potential energy surfaces above the ground state are attainable. The collision is therefore mostly dictated by electron promotion into a σ*(C–Cl) molecular orbital as depicted in Fig. 2 (LUMO+5). Formation of $C_6Cl_5^-$ and/or Cl^- occurs after cleavage of a C–Cl bond in the TNI and results from a complementary reaction with respect to the negative charge:

$$K + C_6Cl_6 \rightarrow (K^+\ C_6Cl_6^-) \rightarrow K^+ + (C_6Cl_6^-)^{\#} \rightarrow K^+ + C_6Cl_5^- + Cl \quad (2)$$

$$K + C_6Cl_6 \rightarrow (K^+\ C_6Cl_6^-) \rightarrow K^+ + (C_6Cl_6^-)^{\#} \rightarrow K^+ + Cl^- + C_6Cl_5 \quad (3)$$

where (C_6Cl_5–Cl) represents a direct bond breaking and the extra charge sitting on one of the radicals, either on $C_6Cl_5^{\bullet}$ or on $Cl^{\bullet}$. Note that the EA(Cl) = 3.6131 eV[45] and the EA(C_6Cl_5) = 3.10 ± 0.24 eV[45] are essentially identical, yet the Cl^- yield is approximately 3 to 4 times higher than $C_6Cl_5^-$ for E_{CM} < 30 eV and 6 to 7 times higher for E_{CM} > 30 eV collision energy (see BRs in Fig. 5). Such behaviour seems plausible given the electronic structure of the hexachlorobenzene molecule. For E_{CM} < 30 eV, the extra electron could attach and occupy the LUMO (Fig. S1) with mostly π_{CC}* character. In such a delocalized system, all six identical chlorine atoms compete for the extra charge, with the excess energy being channelled into the available degrees of freedom, resulting in a stable parent anion rather than prevalent bond breaking. The shape of a selection of $C_6Cl_6^-$ molecular orbitals calculated at the RKS/ B3LYP+D3 level of theory (see Fig. S3) reveal that the SOMO has π_{CCl} character while the next MO shows a strong σ_{CCl}* antibonding nature. Effective bond breaking yielding Cl^- can only be achieved by efficient non-adiabatic curve crossing between π_{CCl}* and σ_{CCl}* (see Fig. S1 and 72, π* and 73, σ_{CCl}* in Fig. S3), providing that the nuclear wave packet in the C–Cl coordinate survives long enough for the system to change its character, resulting in the formation of a chlorine anion. However, as the collision energy is increased, the number of electronic excited states being accessed also increases, the MOs are mostly σ_{CCl}* in character (Fig. S3) and so direct bond cleavage resulting in Cl^- formation is expected to be more favourable. The Cl^- BR in Fig. 5 shows clearly that trending behaviour as the collision energy is increased above E_{CM} = 20 eV. Moreover, in the high energy collision region, one should not discard that such anion formation can also proceed through shape and/or core-excited resonances, the latter e.g. relaxing into a dissociative state by internal conversion.

The K^+ energy loss spectrum obtained in the forward direction, shows the main feature at (8.1 ± 0.2) eV (Fig. 4) with a vertical electron affinity of (–3.76 ± 0.20) eV. This can be

assigned to a purely repulsive transition from C_6Cl_6 ground state to a σ_{CCl}* state of the temporary negative ion yielding Cl^- formation, given that this is the most intense fragment anion formed in potassium–hexachlorobenzene collisions above 10 eV.

The energy loss feature peaking at 6.2 ± 0.3 eV (Fig. 4), results from accessing an electronic state at 1.86 ± 0.30 eV above the neutral molecule. The calculated molecular orbital for hexachlorobenzene anion at 1.92 eV (Fig. S3), shows a remarkable σ_{CCl}* antibonding character with the extra charge sitting on the C_6Cl_5 radical (Fig. S3). If we now take the ionisation energy of the potassium atom as 4.34 eV[45] and the C_6Cl_5 electron affinity (see above), from the appearance energy (*AE*) in the energy loss spectrum (~4.5 eV), we can estimate the C_6Cl_5–Cl bond dissociation energy. Thus, $D(C_6Cl_5\text{–}Cl) = AE(C_6Cl_5^-) - IE(K) + EA(C_6Cl_5) = (3.26 \pm 0.30)$ eV, which is in excellent accord with Yamada and co-workers[19] calculated value of 3.297 eV (318.1 kJ/mol).

4.4 Other fragments

The branching ratios in Fig. 5 show that other fragment anions account for ≤ 20% of the total anion yield and these have been assigned to $C_6Cl_4^-$, $C_3Cl_2^-$, C_2Cl^- and Cl_2^-. The possible reaction mechanisms that can be involved in such anions' formation are:

$$K + C_6Cl_6 \rightarrow (K^+\ C_6Cl_6^-) \rightarrow K^+ + (C_6Cl_6^-)^\# \rightarrow K^+ + C_6Cl_4^- + Cl_2 \quad (4a)$$

$$K + C_6Cl_6 \rightarrow (K^+\ C_6Cl_6^-) \rightarrow K^+ + (C_6Cl_6^-)^\# \rightarrow K^+ + C_6Cl_4^- + Cl + Cl \quad (4b)$$

$$K + C_6Cl_6 \rightarrow (K^+\ C_6Cl_6^-) \rightarrow K^+ + (C_6Cl_6^-)^\# \rightarrow K^+ + C_3Cl_2^- + C_3Cl_4 \quad (5)$$

$$K + C_6Cl_6 \rightarrow (K^+\ C_6Cl_6^-) \rightarrow K^+ + (C_6Cl_6^-)^\# \rightarrow K^+ + C_2Cl^- + C_4Cl_4 + Cl \quad (6)$$

$$K + C_6Cl_6 \rightarrow (K^+\ C_6Cl_6^-) \rightarrow K^+ + (C_6Cl_6^-)^\# \rightarrow K^+ + Cl_2^- + C_6Cl_4 \quad (7)$$

Note that in (4a) and (4b), the loss of two chlorine atoms may proceed through reactions yielding Cl + Cl and/or Cl_2. A literature survey reveals neither information on dissociative electron attachment experiments to hexachlorobenzene nor $C_6Cl_4^-$ electron affinity, so no comparative studies as to such neutral radical formation is possible to establish.

The TOF mass spectrum inset in Fig. 3 shows two weak signals that have been assigned to $C_3Cl_2^-$ and C_2Cl^- with proposed mechanisms in reactions (5) and (6). We note that these anions are only formed at 100 eV collision energy lab frame, the latter has been reported by MacNeil and Thynne[41] in ion-pair formation from ionisation of tetrachloroethylene. Due to the lack of any other relevant information in the literature regarding either resonances from dissociative electron attachment or any gas-phase thermochemistry data, it is impossible to

estimate any thermodynamic thresholds for reactions (5) and (6) producing $C_3Cl_2^-$ and C_2Cl^- and their associated neutral radicals.

Finally, we detain ourselves with Cl_2^- formation from reaction (7) where two C–Cl bonds have to be broken and a molecular chlorine anion has to be formed. From the electron affinity value of Cl_2 to be (2.5 ± 0.2) eV,[45] the above bond dissociation energy $D(C_6Cl_5–Cl)$ = (3.26 ± 0.30) eV, and taking the available data on D(C–Cl) = (3.3 ± 0.3) eV[46] and D(Cl–Cl) = 2.52 eV,[47] after adding the potassium ionisation energy, the appearance energy of reaction (7) is given by:

$$\Delta_f H_g^\circ(Cl_2^-)=D(C_6Cl_5–Cl)+D(C–Cl)–D(Cl–Cl)–EA(Cl_2)+IE(K)=(5.88 \pm 0.30 \text{ eV}) \quad (7.1)$$

In the energy loss data of Fig. 4, the feature peaking at (7.3 ± 0.2 eV), shows an estimated appearance energy of (5.8 ± 0.2) eV, in good agreement with Cl_2^- formation that may result from reaction (7) with a threshold calculated in (7.1).

The K^+ energy loss features at (9.1 ± 0.1) and (12.1 ± 0.1) eV (Fig. 4) with vertical electron affinities of (–4.76 ± 0.10) and (–7.76 ± 0.10) eV are tentatively assigned to core-excited resonances of π* character and Rydberg excitations, respectively (Table 1). The former is closely related to electronic excitation of the neutral molecule at 4.96 eV to $^1B_{1u}$ state,[8] while Robin reports a value of 5.27 eV;[9] the latter can be assigned to the series $n_{Cl} \rightarrow ns$ converging to (e_{1g}^{-1}) at 9.19 eV.[12] Due to the large number of states which occur in this high energy region, Rydberg assignment is rather difficult to perform, so the series are labelled either as (n+1) or (n+2).

5 Conclusions

We have presented a novel comprehensive study on TOF mass spectrometry negative ion formation in neutral potassium atom collisions with neutral hexachlorobenzene molecules in the lab frame energy range from 10 up to 100 eV. The TOF mass spectra are dominated by the undissociated parent anion $C_6Cl_6^-$, and Cl^- and together with $C_6Cl_5^-$ these anions contribute to more than 80% of the ions recorded, where other fragments assigned to $C_6Cl_4^-$, $C_3Cl_2^-$, C_2Cl^- and Cl_2^-, amounting to less than 20% of the total anion yield. Theoretical calculations on the vertical excitation energies were performed at different levels of theory to help us in assigning the electronic transitions.

Potassium cation post-collision energy loss data has been obtained in the forward direction (θ ≅ 0°) at 162.2 eV in the centre-of-mass frame (205 eV lab frame), with a dominant

feature assigned to an electronic transition with a vertical electron affinity of (–3.76 ± 0.20) eV. This has been assigned to a purely repulsive transition from C_6Cl_6 ground state to a σ_{CCl}*state of the temporary negative ion yielding Cl^- formation. The energy loss data has revealed a weak feature at (3.1 ± 0.3) eV, yielding a positive electron affinity of (1.24 ± 0.3) eV, where its lower lower limit value (0.94 eV) was assigned to C_6Cl_6 adiabatic electron affinity and is in very good agreement with the values reported in the literature. Moreover, the $C_6Cl_5^-$ and Cl_2^- thresholds of formation have been obtained from the experimental energy loss data, the former allowing to estimate a bond dissociation energy $D(C_6Cl_5–Cl)$ = (3.26 ± 0.30) eV.

Conflicts of interest

There are no conflicts to declare.

Acknowledgments

SK acknowledges the Portuguese National Funding Agency (FCT) through PD/BD/142831/2018, and together with PLV the research grants CEFITEC (UIDB/00068/2020) and PTDC/FIS-AQM/31281/2017. This work was also supported by Radiation Biology and Biophysics Doctoral Training Programme (RaBBiT, PD/00193/2012); UCIBIO (UIDB/04378/2020). All the calculations were performed at the CI TASK Computer Centre in Gdańsk. The work of MŁ is based upon support from COST Action CA18212 - Molecular Dynamics in the GAS phase (MD-GAS). GG acknowledges partial financial support from the Spanish Ministerio de Ciencia e Innovación (Project No. PID2019-104727RB-C21) and CSIC (Project LINKA20085).

Supplementary information

The supplementary information provides figures S1 to S3 and tables S1 to S3 with the results of theoretical calculations for a selection of K + C_6Cl_6, C_6Cl_6 Highest Occupied Molecular Orbitals (HOMOs) and Lowest Unoccupied Molecular Orbitals (LUMOs), as well as ionisation energies, electron affinities and vertical detachment energies.

Author information

Sarvesh Kumar; orcid.org/0000-0002-1996-9925

Tymon Kilich; orcid.org/0000-0001-6831-694X

Marta Łabuda; orcid.org/0000-0003-0490-7294
Gustavo García; orcid.org/0000-0003-4033-4518
Paulo Limão-Vieira; orcid.org/0000-0003-2696-1152

References

1 W. W. Brubaker and R. A. Hites, Experimental Section, *Environ. Sci. Technol.*, 1998, **32**, 766–769.

2 M. P. Ormad, N. Miguel, A. Claver, J. M. Matesanz and J. L. Ovelleiro, Pesticides removal in the process of drinking water production, *Chemosphere*, 2008, **71**, 97–106.

3 *Toxicologic profile of hexachlorobenzene, U.S. Department of Health and Human Services, Public Health Service, Agency for Toxic Substances and Disease Registry, Division of Toxicology and Human Health Sciences, Environmental Toxicology Branch*, Atlanta, Georgia, 2015.

4 S. L. Simonich and R. A. Hites, Global distribution of persistent organochlorine compounds, *Science (80-.).*, 1995, **269**, 1851–1854.

5 G. W. Patton, M. D. Walla, T. F. Bidleman and L. A. Barrie, Polycyclic aromatic and organochlorine compounds in the atmosphere of northern Ellesmere Island, Canada, *J. Geophys. Res.*, 1991, **96**, 10867–10877.

6 M. Oehme, Further evidence for long-range air transport of polychlorinated aromates and pesticides: North America and Eurasia to the Arctic, *Ambio.*, 1991, **20**, 293–297.

7 P. Roche and M. Prados, Removal of Pesticides by Use of Ozone or Hydrogen Peroxide/Ozone, *Ozone Sci. Eng.*, 1995, **17**, 657–672.

8 H. Scharping, C. Zetzsch and H. A. Dessouki, The UV absorption spectra of the trichlorobenzenes and the higher chlorinated benzenes in the gas phase and in n-hexane solution, *J. Mol. Spectrosc.*, 1987, **123**, 382–391.

9 M. B. Robin, *Higher Excited States of Polyatomic Molecules, Volume II*, Academic Press, 1975.

10 S. Saëki, The Assignment of the Molecular Vibrations of Hexachlorobenzene, *Bull. Chem. Soc. Jpn.*, 1962, **35**, 322–326.

11 J. R. Scherer and J. C. Evans, Vibrational spectra and assignments for sixteen chlorobenzenes, *Spectrochim. Acta*, 1963, **19**, 1739–1775.

12 B. Ruščić, L. Klasinc, A. Wolf and J. V. Knop, Photoelectron spectra of and ab initio calculations on chlorobenzenes. 3. Hexachlorobenzene, *J. Phys. Chem.*, 1981, **85**, 1495–1497.

13 W. B. Knighton, J. A. Bognar and E. P. Grimsrud, Reactions of Selected Molecular Anions with Oxygen, *J. Mass Spectrom.*, 1995, **30**, 557–562.

14 P. P. Romańczyk, G. Rotko and S. S. Kurek, Dissociative electron transfer in polychlorinated aromatics. Reduction potentials from convolution analysis and quantum chemical calculations, *Phys. Chem. Chem. Phys.*, 2016, **18**, 22573–22582.

15 T. Kato and T. Yamabe, Vibronic interactions and charge transfer in negatively charged chloroacenes, *Chem. Phys.*, 2006, **321**, 149–158.

16 V. K. Voora, Molecular Electron Affinities Using the Generalized Kohn-Sham Semicanonical Projected Random Phase Approximation, *J. Phys. Chem. Lett.*, 2021, **12**, 433–439.

17 J. R. Wiley, E. C. M. Chen, E. S. D. Chen, P. Richardson, W. R. Reed and W. E. Wentworth, The determination of absolute electron affinities of chlorobenzenes, chloronaphthalenes and chlorinated biphenyls from reduction potentials, *J. Electroanal. Chem.*, 1991, **307**, 169–182.

18 W. Xu and A. Gao, DFT study on the electron affinities of the chlorinated benzenes, *J. Mol. Struct.-Theochem*, 2005, **732**, 63–70.

19 S. Yamada, Y. Naito, M. Takada, S. Nakai and M. Hosomi, Photodegradation of hexachlorobenzene and theoretical prediction of its degradation pathways using quantum chemical calculation, *Chemosphere*, 2008, **70**, 731–736.

20 R. Antunes, D. Almeida, G. Martins, N. J. Mason, G. Garcia, M. J. P. Maneira, Y.

Nunes and P. Limão-Vieira, Negative ion formation in potassium–nitromethane collisions, *Phys. Chem. Chem. Phys.*, 2010, **12**, 12513–12519.

21 K. Regeta, S. Kumar, T. Cunha, M. Mendes, A. I. Lozano, P. J. S. Pereira, G. García, A. M. C. Moutinho, M. C. Bacchus-Montabonel and P. Limão-Vieira, Combined Experimental and Theoretical Studies on Electron Transfer in Potassium Collisions with CCl4, *J. Phys. Chem. A*, 2020, **124**, 3220–3227.

22 E. Bene, Á. Vibók, G. J. Halász and M. C. Bacchus-Montabonel, Ab initio molecular treatment of charge transfer processes induced by collision of C2+ ions with the OH radical: A linear approach, *Chem. Phys. Lett.*, 2008, **455**, 159–163.

23 M. C. Bacchus-Montabonel and Y. S. Tergiman, Radiation damage on biomolecular systems : Dynamics of ion induced collision processes, *Comput. Theor. Chem*, 2012, **990**, 177–184.

24 M. C. Bacchus-Montabonel and Y. S. Tergiman, Charge transfer dynamics of carbon ions with uracil and halouracil targets at low collision energies, *Chem. Phys. Lett.*, 2011, **503**, 45–48.

25 M. C. Bacchus-Montabonel, M. Łabuda, Y. S. Tergiman and J. E. Sienkiewicz, Theoretical treatment of charge-transfer processes induced by collision of Cq+ ions with uracil, *Phys. Rev. A*, 2005, **72**, 052706.

26 E. Erdmann, M.-C. Bacchus-Montabonel and M. Łabuda, Modelling charge transfer processes in C2+-tetrahydrofuran collision for ion-induced radiation damage in DNA building blocks, *Phys. Chem. Chem. Phys.*, 2017, **19**, 19722–19732.

27 M. Mendes, B. Pamplona, S. Kumar, F. F. da Silva, A. Aguilar, G. García, M. C. Bacchus-Montabonel and P. Limão-Vieira, Ion-pair formation in neutral potassium-neutral pyrimidine collisions: Electron transfer experiments, *Front. Chem.*, 2019, **7**, 1–10.

28 D. Almeida, M.-C. Bacchus-Montabonel, F. Ferreira da Silva, G. García and P. Limão-Vieira, Potassium-uracil/thymine ring cleavage enhancement as studied in electron transfer experiments and theoretical calculations, *J. Phys. Chem. A*, 2014, **118**, 6547–6552.

29 L. Salem, *Electrons in Chemical Reactions: First Principles*, Wiley Interscience: New York, 1982.

30 M. C. Bacchus-Montabonel and Y. S. Tergiman, An ab initio study of ion induced charge transfer dynamics in collision of carbon ions with thymine, *Phys. Chem. Chem. Phys.*, 2011, **13**, 9761–9767.

31 M. C. Bacchus-Montabonel, Ab Initio Treatment of Ion-Induced Charge Transfer Dynamics of Isolated 2 - Deoxy - D - ribose, *J. Phys. Chem. A*, 2014, **118**, 6326–6332.

32 M. C. Bacchus-Montabonel and F. Calvo, Nanohydration of uracil: Emergence of three-dimensional structures and proton-induced charge transfer, *Phys. Chem. Chem. Phys.*, 2015, **17**, 9629–9633.

33 A. Schäfer, C. Huber and R. Ahlrichs, Fully optimized contracted Gaussian basis sets of triple zeta valence quality for atoms Li to Kr, *J. Chem. Phys.*, 1994, **100**, 5829–5835.

34 F. Neese, The ORCA program system, *Wiley Interdiscip. Rev. Comput. Mol. Sci.*, 2012, **2**, 73–78.

35 H.-J. Werner, P. J. Knowles, G. Knizia, F. R. Manby and M. Schütz, Molpro: A general-purpose quantum chemistry program package, *Wiley Interdiscip. Rev. Comput. Mol. Sci.*, 2012, **2**, 242–253.

36 A. Nicklass, M. Dolg, H. Stoll and H. Preuss, Ab initio energy-adjusted pseudopotentials for the noble gases Ne through Xe: Calculation of atomic dipole and quadrupole polarizabilities, *J. Chem. Phys.*, 1995, **102**, 8942–8952.

37 B. O. Roos, *Ab initio methods in Quantum Chemistry II*, Wiley-VCH, Chichester, 1987.

38 H. J. Werner and P. J. Knowles, A second order multiconfiguration SCF procedure with optimum convergence, *J. Chem. Phys.*, 1985, **82**, 5053–5063.

39 P. J. Knowles and H. J. Werner, An efficient second-order MC SCF method for long configuration expansions, *Chem. Phys. Lett.*, 1985, **115**, 259–267.

40 S. Grimme, J. Antony, S. Ehrlich and H. Krieg, A consistent and accurate ab initio parametrization of density functional dispersion correction (DFT-D) for the 94 elements H-Pu, *J. Chem. Phys.*, 2010, **132**, 154104.

41 P. Limão-Vieira, A. M. C. Moutinho and J. Los, Dissociative ion-pair formation in collisions of fast potassium atoms with benzene and fluorobenzene, *J. Chem. Phys.*, 2006, **124**, 054306.

42 A. W. Kleyn and A. M. C. Moutinho, Negative ion formation in alkali-atom – molecule, *J. Phys. B At. Mol. Opt. Phys.*, 2001, **4075**, R1–R44.

43 M. Mendes, M. Probst, T. Maihom, G. García and P. Limão-Vieira, Selective Bond Excision in Nitroimidazoles by Electron Transfer Experiments, *J. Phys. Chem. A*, 2019, **123**, 4068–4073.

44 M. Mendes, G. García, M. C. Bacchus-Montabonel and P. Limão-Vieira, Electron transfer induced decomposition in potassium–nitroimidazoles collisions: An experimental and theoretical work, *Int. J. Mol. Sci.*, 2019, **20**, 6170.

45 http://webbook.nist.gov/chemistry/, http://webbook.nist.gov/chemistry/.

46 E. Illenberger, Energetics of Negative Ion Formation in Dissociative Electron Attachment to CCl4, CFCl3, CF2Cl2, and CF3Cl, *Ber. Bunsenges. Phys. Chem.*, 1982, **86**, 252–261.

47 H.-U. Scheunemann, E. Illenberger and H. Baumgartel, Dissociative Electron

Attachment to CCl4, CHCl3, CH2C12 and CH3Cl, *Ber. Bunsenges. Phys. Chem.*, 1980, **84**, 580–585.

Fig. 1. Molecular structure of C_6Cl_6 and orientation of the K–C_6Cl_6 collisional system; *K*, purple, *x*, red; *y*, green; *z*, blue.

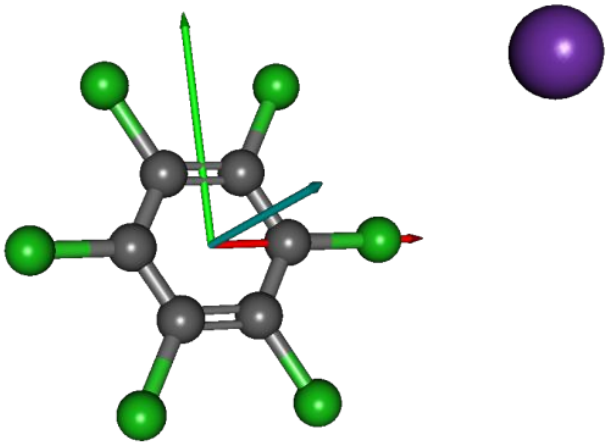

Fig. 2. Calculated highest occupied molecular orbitals (HOMOs) and lowest unoccupied molecular orbitals (LUMOs) for C_6Cl_6 and K + C_6Cl_6. Energies in eV.

	C_6Cl_6	K + C_6Cl_6
HOMOs	$\bar{n}_{Cl}$ (in-plane) -11.9 eV 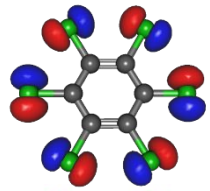 π_{CCl} -10.5 eV 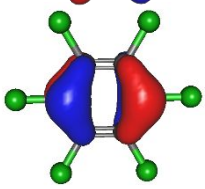	$\bar{n}_{Cl}$ (in-plane) -12.0 eV 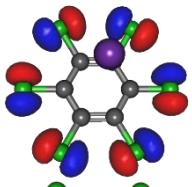 π_{CC} -10.6 eV 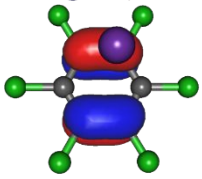
LUMOs	π_{CC}* 2.89 eV 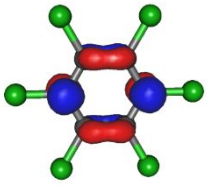	π_{CC}* 2.89 eV 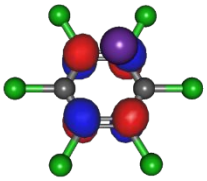
	π_{CC}* 2.96 eV 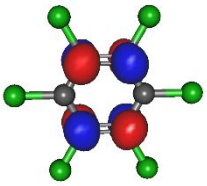	π_{CC}*/σ_{CC}* + σ_{CCl}* 3.09 eV 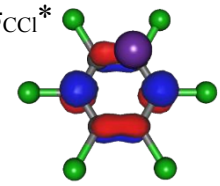
	π_{CC}* 9.72 eV 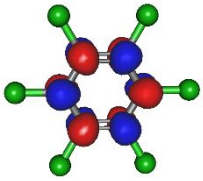	π_{CC}* 9.84 eV 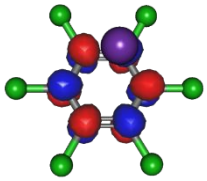
	σ_{CC}* 17.0 eV 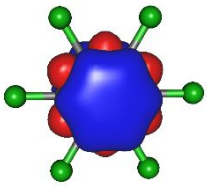	σ_{CC}* 15.8 eV 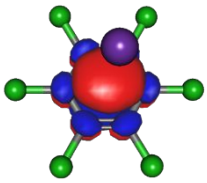
	σ_{CC}* 17.2 eV 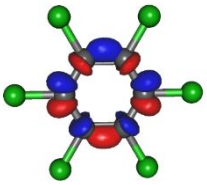	σ_{CC}* 16.2 eV 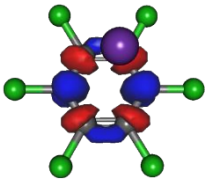
	σ_{CC}* 17.5 eV 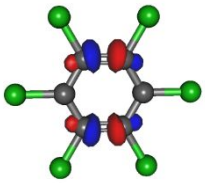	σ_{CC}*+ σ_{CCl}* 16.6 eV 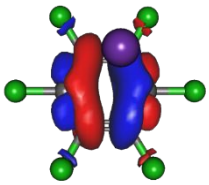

Fig. 3. Time-of-flight negative ion mass spectra in potassium (K)–hexachlorobenzene (C_6Cl_6) collisions at 100 eV lab frame energy (79.1 eV in the centre-of-mass frame). See text for details.

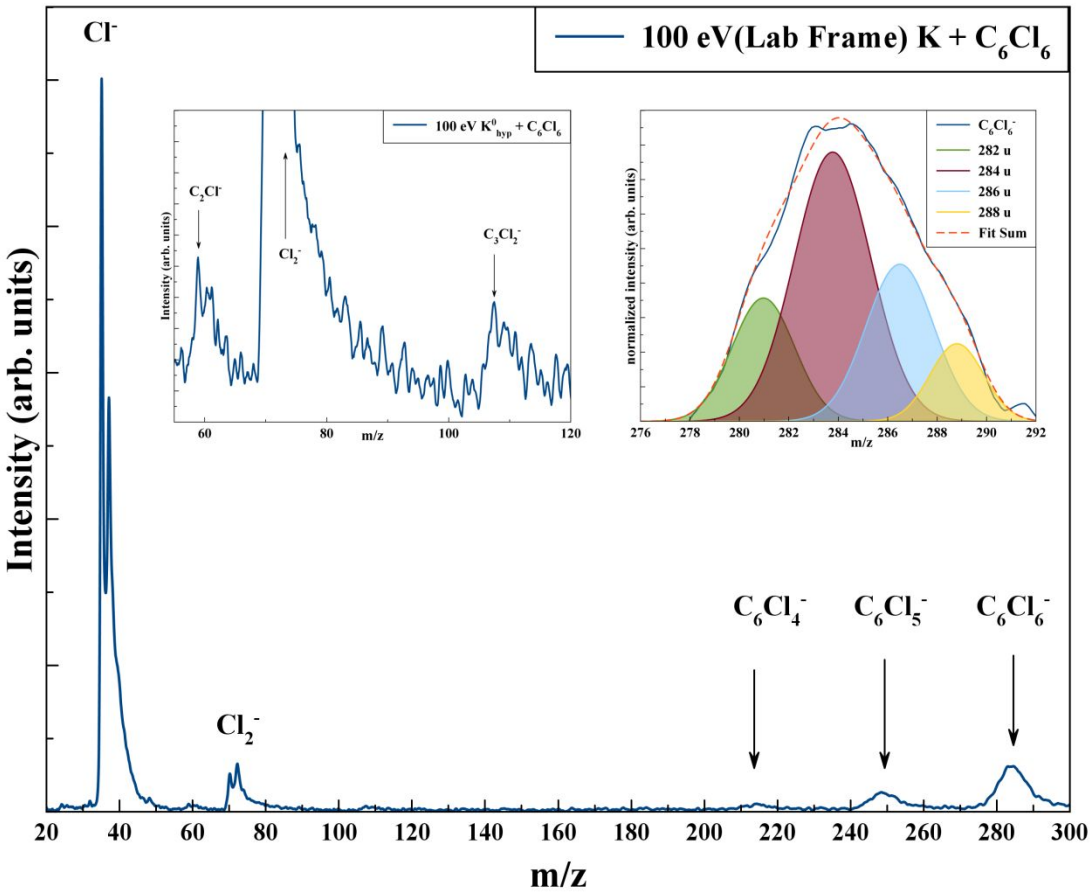

Fig. 4. Energy loss spectrum of K^+ ions formed in the forward direction of K atoms in collisions with C_6Cl_6 at 205 eV lab frame energy (162 eV in the centre-of-mass frame). See text for details. Error bars are within experimental data points and within 10% associated with the fitting.

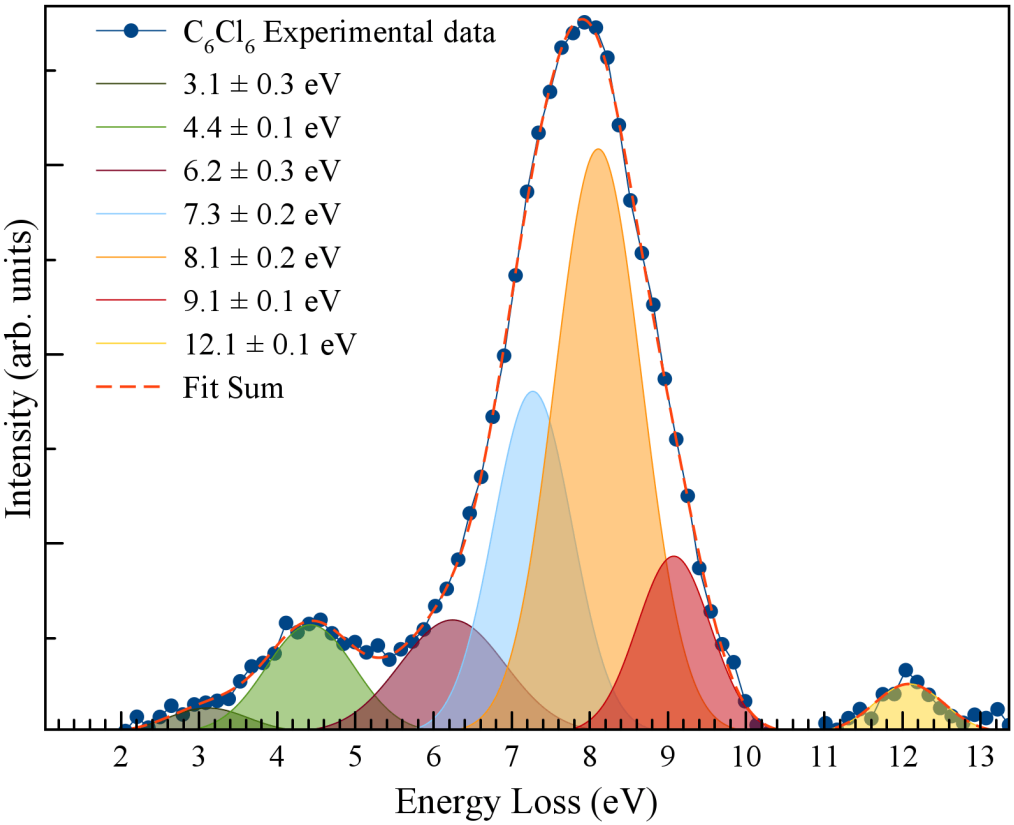

Fig. 5. Hexachlorobenzene (C_6Cl_6) branching ratios (fragment anion yield/total anion yield) of the main negative ions formed as a function of the collision energy in the centre-of-mass frame. Error bars related to the experimental uncertainty associated with the ion yields have been added to a few data points in order to avoid congestion of the figure. The lines are just to guide the eye. See text for details.

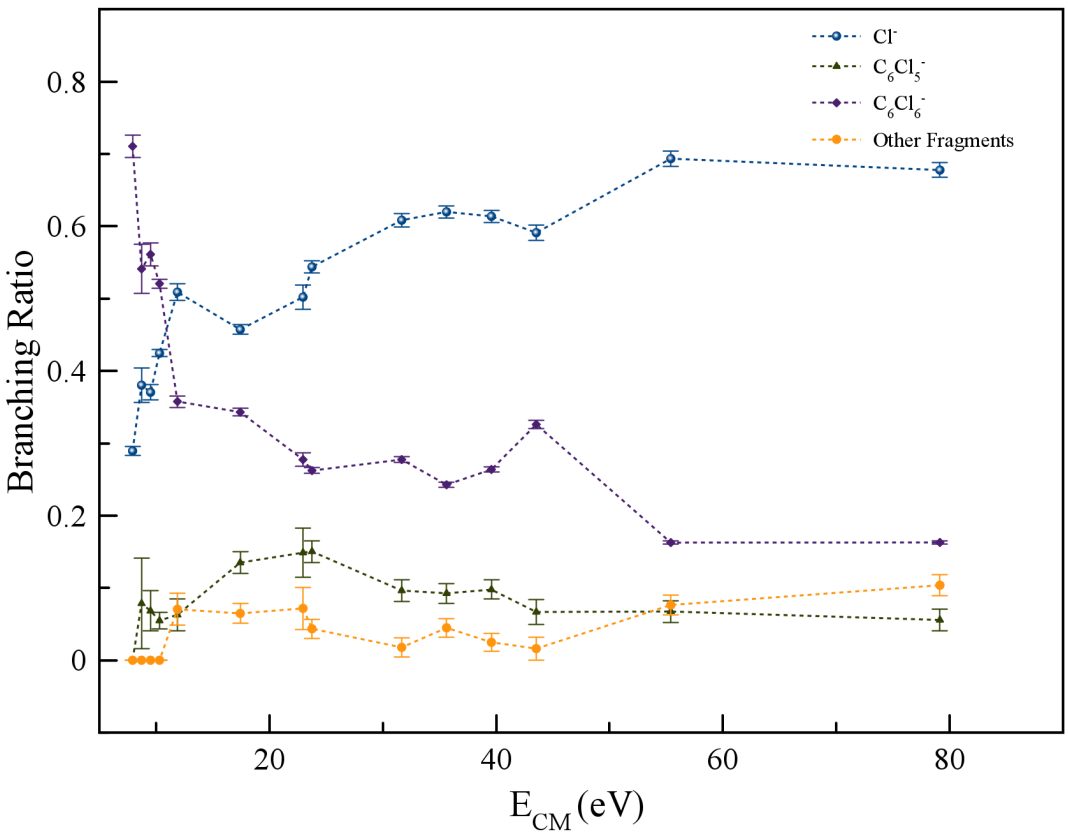

Table 1. Assignment of different features from Gaussian fitting to K^+ energy loss spectrum from potassium collisions with hexachlorobenzene 205 eV lab frame energy (162 eV in the centre-of-mass frame). The uncertainties result from the Gaussian fitting procedure. See text for details.

K^+ Energy Loss Features (eV)	Vertical Electron Affinity (eV)	Calculated Vertical Energy of MO (eV)	Assignment	Ref.[16]	Adiabatic Electron Affinity (eV)[13,17]
3.1 ± 0.3	1.24 ± 0.30	0.98[a]			0.91; 0.98
4.4 ± 0.1	–0.06 ± 0.10		π^*	vb[b]-π^*	
6.2 ± 0.3	–1.86 ± 0.30	–1.92	71, σ_{CCl}^*		
7.3 ± 0.2	–2.96 ± 0.20	–3.10	LUMO+1		
8.1 ± 0.2	–3.76 ± 0.20		σ_{CCl}^*		
9.1 ± 0.1	–4.76 ± 0.10		π^*		
12.1 ± 0.1	–7.76 ± 0.10		$n_{Cl} \rightarrow (n+1)s$ $n_{Cl} \rightarrow (n+2)s$		

[a] adiabatic electron affinity;

[b] valence-bound state, with calculated electron affinities of 0.03 eV (aug-cc-pVDZ+7S7P), 0.30 eV (aug-cc-pVTZ+7S7P) and 0.29 eV(aug-cc-pVTZ). See Voora[16] for details.

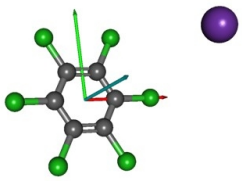

Molecular structure of C6Cl6 and orientation of the K–C6Cl6 collisional system; K, purple, x, red; y, green; z, blue.

338x190mm (96 x 96 DPI)

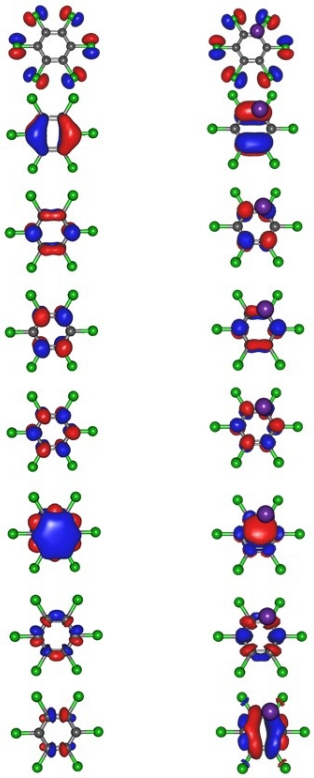

Calculated highest occupied molecular orbitals (HOMOs) and lowest unoccupied molecular orbitals (LUMOs) for C6Cl6 and K + C6Cl6. Energies in eV.

190x338mm (96 x 96 DPI)

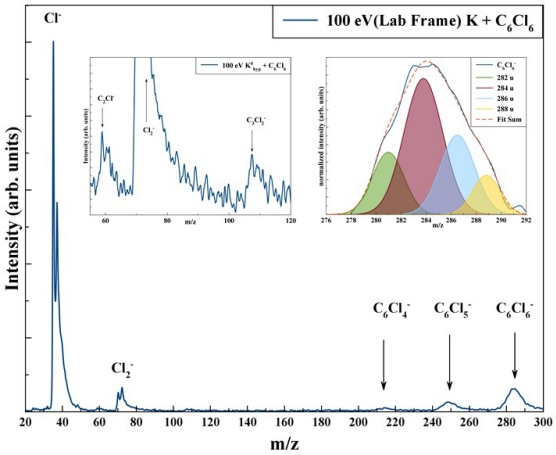

Time-of-flight negative ion mass spectra in potassium (K)–hexachlorobenzene (C6Cl6) collisions at 100 eV lab frame energy (79.1 eV in the centre-of-mass frame). See text for details.

338x190mm (96 x 96 DPI)

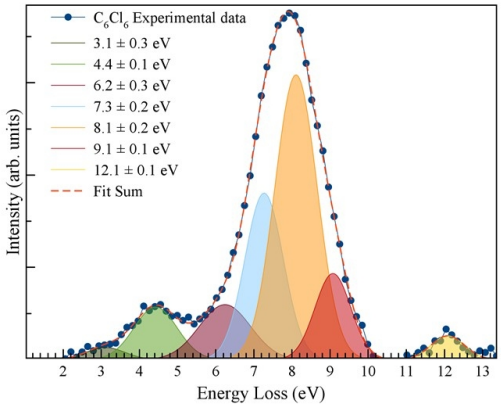

Energy loss spectrum of K+ ions formed in the forward direction of K atoms in collisions with C6Cl6 at 205 eV lab frame energy (162 eV in the centre-of-mass frame). See text for details. Error bars are within experimental data points and within 10% associated with the fitting.

338x190mm (96 x 96 DPI)

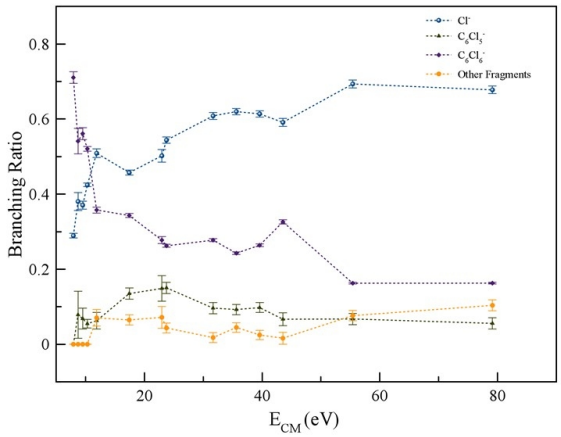

Hexachlorobenzene (C6Cl6) branching ratios (fragment anion yield/total anion yield) of the main negative ions formed as a function of the collision energy in the centre-of-mass frame. Error bars related to the experimental uncertainty associated with the ion yields have been added to a few data points in order to avoid congestion of the figure. The lines are just to guide the eye. See text for details.

338x190mm (96 x 96 DPI)

Effective bond breaking in electron transfer from K collisions with C_6Cl_6)

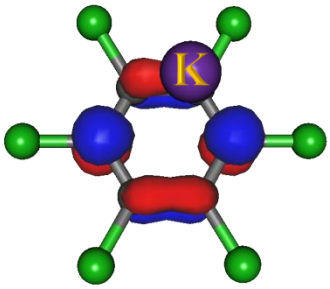

Supplementary Information

Anionic states of C_6Cl_6 probed in electron transfer experiments

S. Kumar[1], T. Kilich[2], M. Łabuda[2], G. García[3], and P. Limão-Vieira[1,a)]

[1] Atomic and Molecular Collisions Laboratory, CEFITEC, Department of Physics, Universidade NOVA de Lisboa, 2829-516 Caparica, Portugal

[2] Department of Theoretical Physics and Quantum Information, Gdańsk University of Technology, Narutowicza 11/12, 80-233 Gdańsk, Poland

[3] Instituto de Física Fundamental, Consejo Superior de Investigaciones Científicas (CSIC), Serrano 113-bis, 28006 Madrid, Spain

Hexachlorobenzene molecule was considered in the D_{2h} symmetry for benchmarking the calculations and choice of the molecular framework. Then, the geometry of the ground S_0 $^1A'$ singlet state of C_6Cl_6 was considered to be of C_{2v} symmetry and has been optimized by means of Møller-Plesset perturbation theory (MP2) calculations with the balanced polarized triple-zeta def2-TZVP basis set[1] which has been shown to be computationally efficient and provides accurate structures and transition energies. All calculations have been performed using the ORCA and MOLPRO packages of *ab initio* programmes.[2,3] The energy of the optimized molecule is E_{MP2} = -2986.35880 a.u. The HOMO is located at $20b_1$ with an energy E_{HOMO} = -9.68 eV and the LUMO at $22a_1$ with an energy E_{LUMO} = 1.83 eV. The LUMO-HOMO energy difference is 11.51 eV.

Figure caption

FIG. S1. Selection of the molecular orbitals for K + C_6Cl_6 (K: magenta, C: grey, Cl: green) at CAS(13,16). See also Table S1.

FIG. S2. Selection of the molecular orbitals for C_6Cl_6 (C: grey, Cl: green) at CAS(12,12). See also Table S2.

FIG. S3. $C_6Cl_6^-$ molecular orbitals: the highest doubly occupied (68-69), singly occupied (70, SOMO) as well as the lowest unoccupied (71-73) (RKS, B3LYP+D3) (C: grey, Cl: green).

FIG. S4. TOF mass spectrum of Cl_2^- anion at 100 eV collision energy and fitted with functions to reproduce its isotope contributions at 70 u (100%), 72 u (~65%) and 74 u (~15%).

Table caption

Table S1. Character and energy of calculated molecular orbitals for K + C_6Cl_6 with an active space CAS(13,16) at the MP2/def2-TZVP level of theory in C_{2v} symmetry.

Table S2. Character and energy of calculated molecular orbitals for C_6Cl_6 with an active space CAS(12,12) at the MP2/def2-TZVP level of theory in C_{2v} symmetry.

Table S3. Adiabatic and vertical ionisation energies, adiabatic and vertical electron affinities and vertical detachment energy (VDE) for C_6Cl_6 geometry optimized at RKS/B3LYP+D3/aug-cc-pVTZ level.

Table S4. Calculated energies (in a.u.) of the neutral, anion and cation of C_6Cl_6 at geometries of neutral and ionized system using RKS/B3LYP+D3/aug-cc-pVTZ for RHF-SCF, RMP2, and RKS methods.

FIG. S1. Selection of the molecular orbitals for K + C_6Cl_6 (K: magenta, C: grey, Cl: green) at CAS(13,16). See also Table S1.

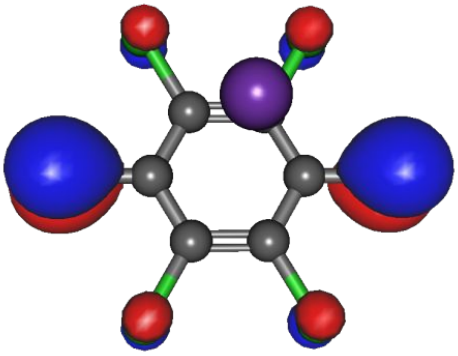	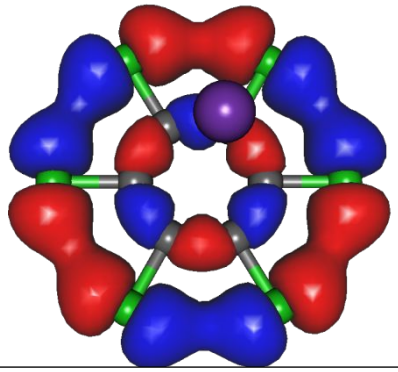
HOMO-7, n_{Cl} (out-of-plane)	HOMO-6
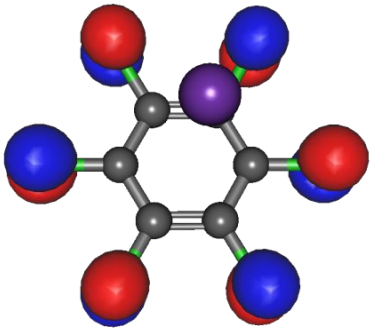	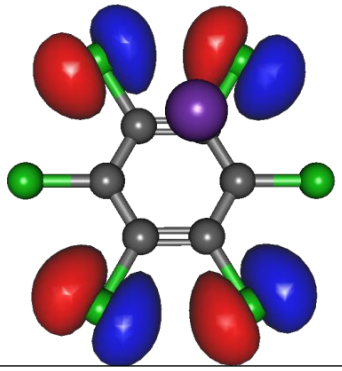
HOMO-5, n_{Cl} (out-of-plane)	HOMO-4, $\bar{n}_{Cl}$ (in-plane)
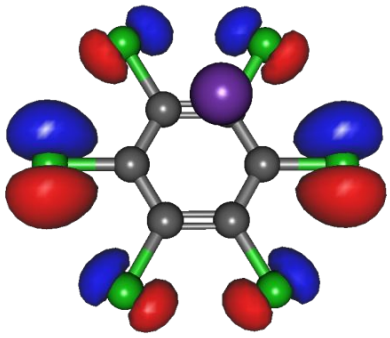	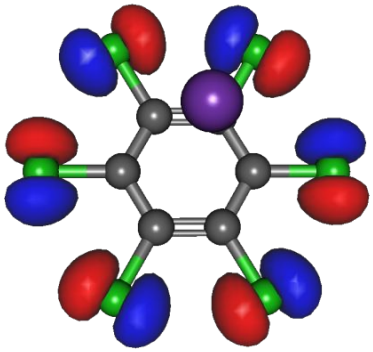
HOMO-3, $\bar{n}_{Cl}$ (in-plane)	HOMO-2, $\bar{n}_{Cl}$ (in-plane)
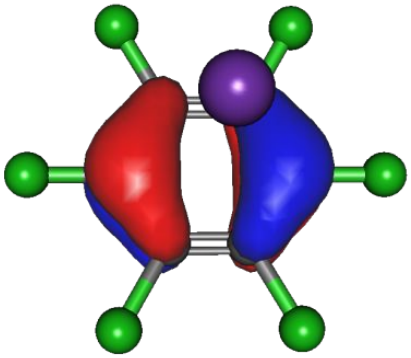	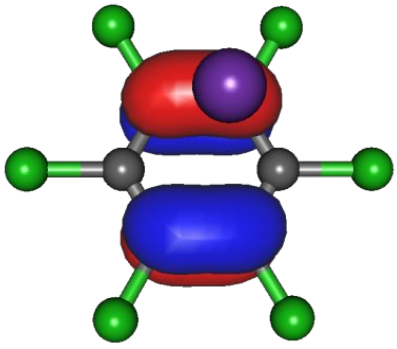
HOMO-1, π_{CCl}	HOMO, π_{CC}

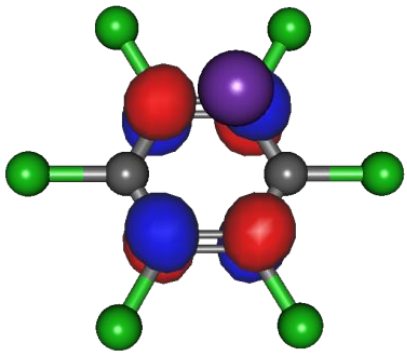	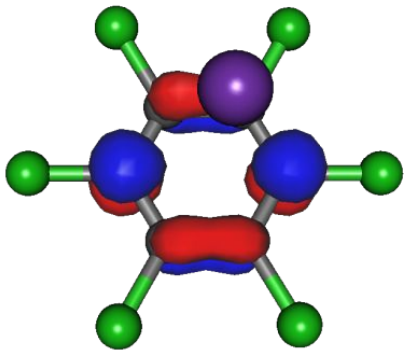
LUMO, π_{CC}*	LUMO+1, π_{CC}*/σ_{CC}* + σ_{CCl}*
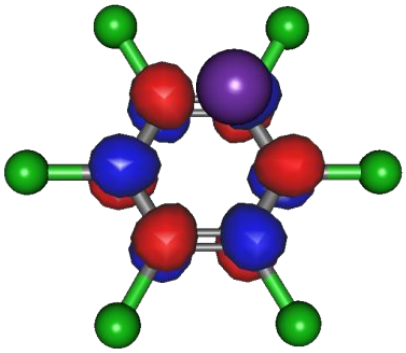	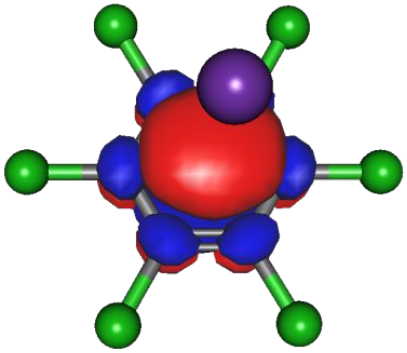
LUMO+2, π_{CC}*	LUMO+3, σ_{CC}*
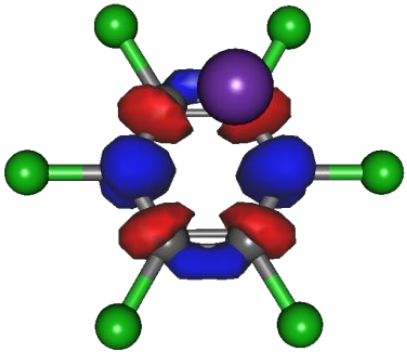	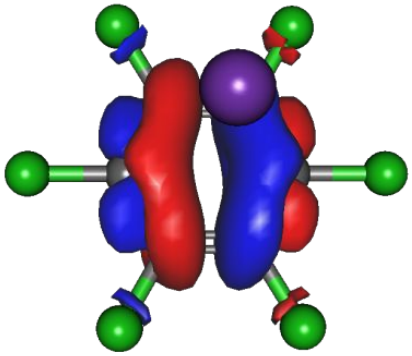
LUMO+4, σ_{CC}*	LUMO+5, σ_{CC}* + σ_{CCl}*
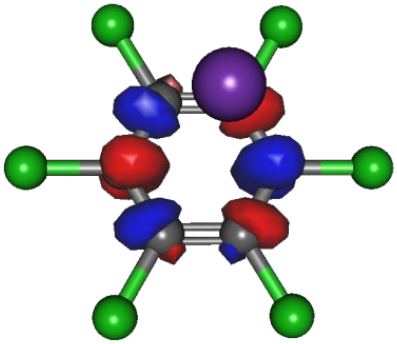	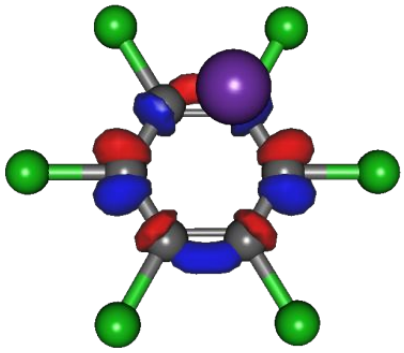
LUMO+6, σ_{CC}*	LUMO+7, σ_{CC}*

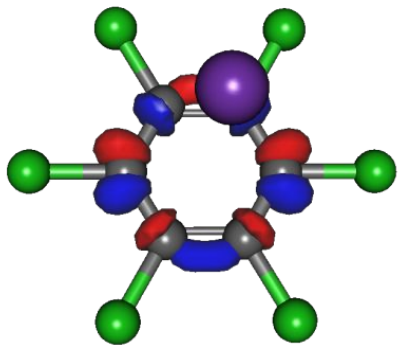	
LUMO+8, σ_{CC}*	

FIG. S2. Selection of the molecular orbitals for C_6Cl_6 (C: grey, Cl: green) at CAS(12,12). See also Table S2.

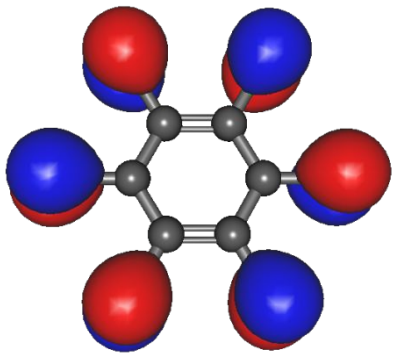	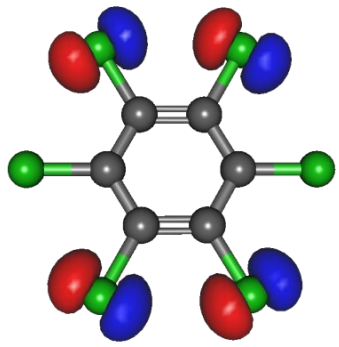
HOMO-5, n_{Cl} (out-of-plane)	HOMO-4, $\bar{n}_{Cl}$ (in-plane)
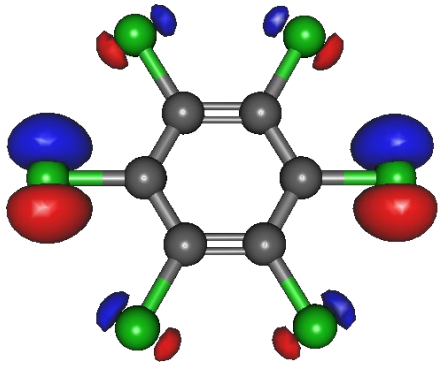	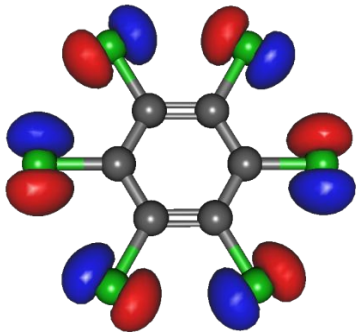
HOMO-3, $\bar{n}_{Cl}$ (in-plane)	HOMO-2, $\bar{n}_{Cl}$ (in-plane)
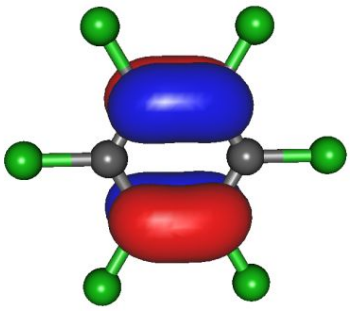	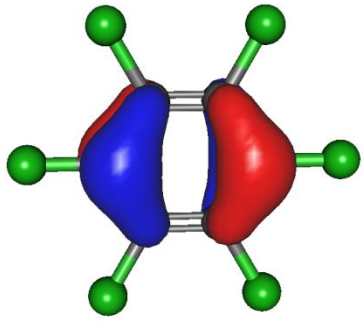
HOMO-1, π_{CC}	HOMO, π_{CCl}
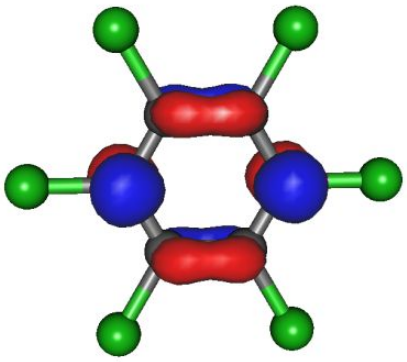	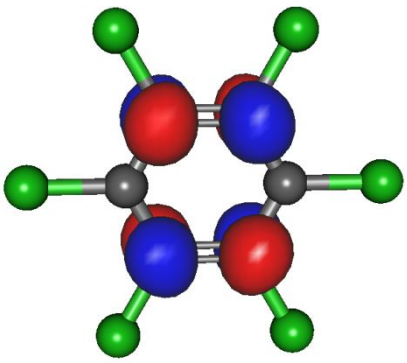
LUMO, $\pi_{CC}^*/\sigma_{CC}^* + \sigma_{CCl}^*$	LUMO+1, π_{CC}^*

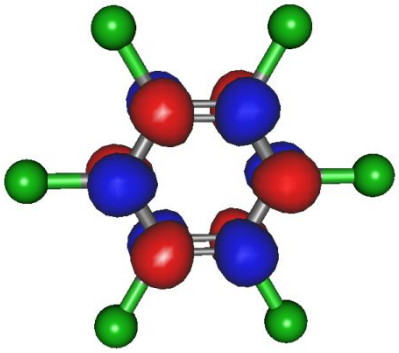	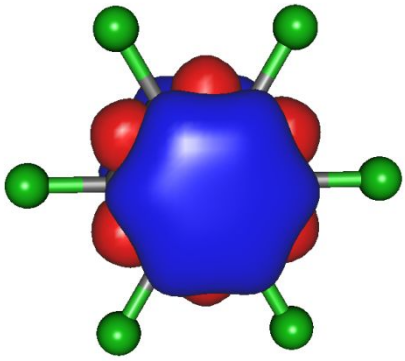
LUMO+2, π_{CC}*	LUMO+3, σ_{CC}*
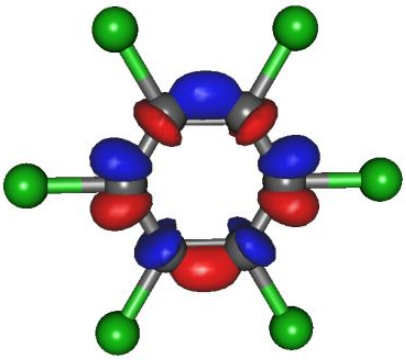	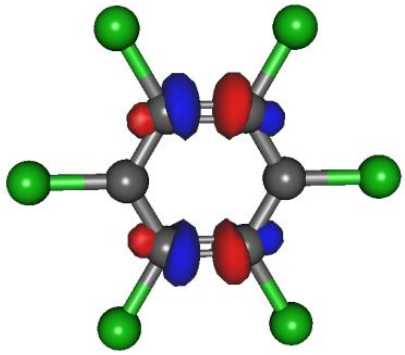
LUMO+4, σ_{CC}*	LUMO+5, π_{CC}* + σ_{CC}*

FIG. S3. $C_6Cl_6^-$ molecular orbitals: the highest doubly occupied (68-69), singly occupied (70, SOMO) as well as the lowest unoccupied (71-73) (RKS, B3LYP+D3) (C: grey, Cl: green).

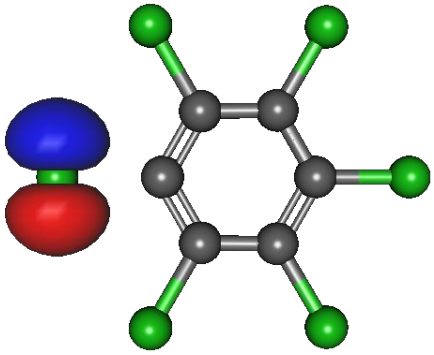	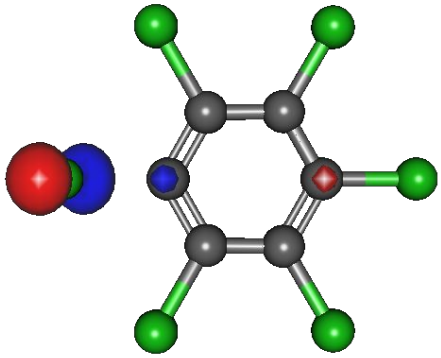
68, π (-3.366 eV)	69, π (-3.148 eV)
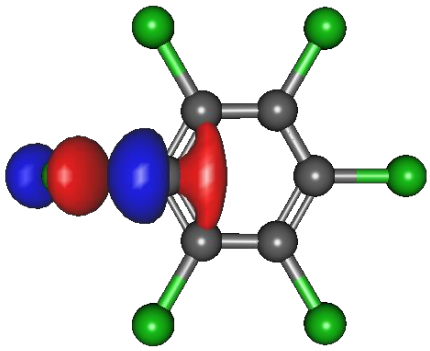	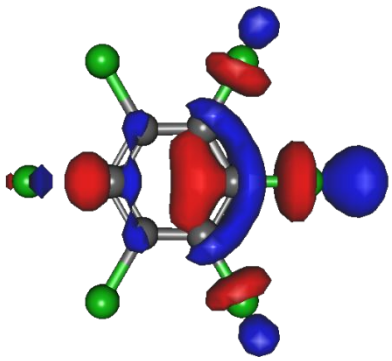
70, SOMO, π_{CCl} (-1.096 eV)	71, σ_{CCl}* (1.918 eV)
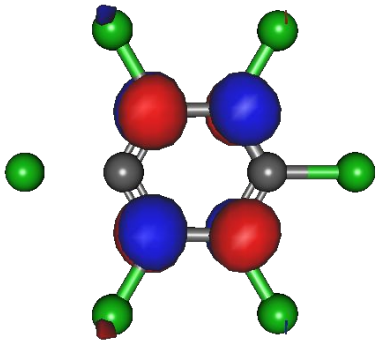	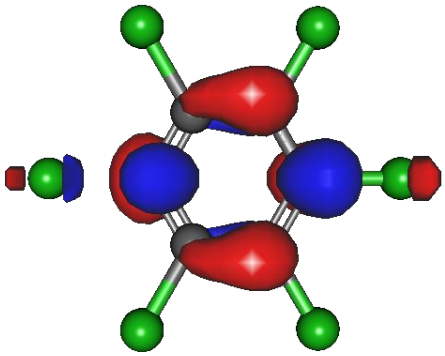
72, π* (2.174 eV)	73, σ_{CCl}* (2.435 eV)

FIG. S4. TOF mass spectrum of Cl_2^- anion at 100 eV collision energy and fitted with functions to reproduce its isotope contributions at 70 u (100%), 72 u (~65%) and 74 u (~15%).

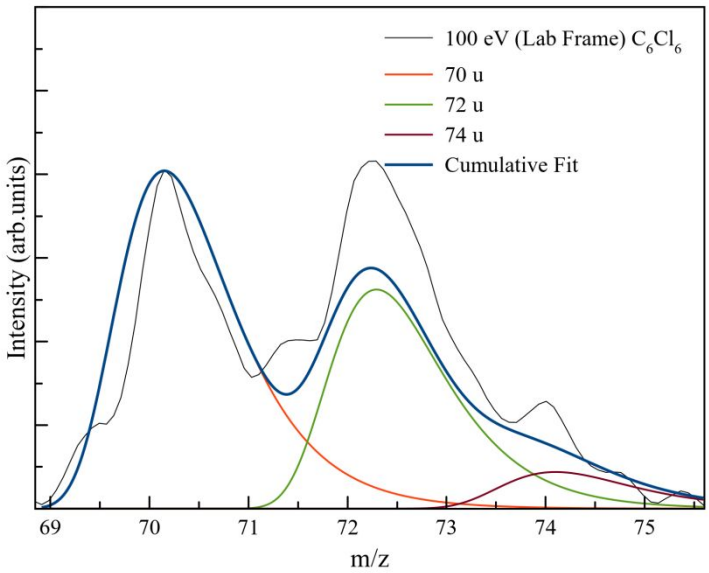

Table S1. Character and energy of calculated molecular orbitals for K + C_6Cl_6 with an active space CAS(13,16) at the MP2/def2-TZVP level of theory in C_{2v} symmetry.

Character	Energy (a.u.)	Energy (eV)
HOMO-2	-0.4420	-12.027
HOMO-1	-0.3903	-10.621
HOMO	-0.3884	-10.569
SOMO	-0.0604	-1.644
LUMO	0.1061	2.887
LUMO+1	0.1138	3.097
LUMO+2	0.3617	9.842
LUMO+3	0.5812	15.815
LUMO+4	0.5946	16.180
LUMO+5	0.6113	16.634
LUMO+6	0.6537	17.788
LUMO+7	0.6746	18.357
LUMO+8	0.9701	26.398

Table S2. Character and energy of calculated molecular orbitals for C_6Cl_6 with an active space CAS(12,12) at the MP2/def2-TZVP level of theory in C_{2v} symmetry.

Character	Energy (a.u)	Energy (eV)
HOMO-4	-0.4734	-12.882
HOMO-3	-0.4734	-12.882
HOMO-2	-0.4404	-11.984
HOMO-1	-0.3860	-10.504
HOMO	-0.3848	-10.471
LUMO	0.1059	2.882
LUMO+1	0.1090	2.966
LUMO+2	0.3571	9.717
LUMO+3	0.6252	17.013
LUMO+4	0.6310	17.170
LUMO+5	0.6428	17.491

Table S3. Adiabatic and vertical ionisation energies, adiabatic and vertical electron affinities and vertical detachment energy (VDE) for C_6Cl_6 geometry optimized at RKS/B3LYP+D3/aug-cc-pVTZ level.

Method	**Ionisation energy (eV)**		**Electron affinity (eV)**			**Vertical detachment energy (eV)**
	adiabatic	vertical	adiabatic	vertical	exp.	
RKS, B3LYP+D3[4]	-	9.00 9.19[5]	0.95	0.38	0.91[6] 0.98[7]	2.70
RKS, B3LYP	-	9.0	0.94	0.38		2.70
RMP2	-	9.45	0.50	0.01		2.56
RHF-SCF	-	8.93	-0.07	-1.16		2.19

Table S4. Calculated energies (in a.u.) of the neutral, anion and cation of C_6Cl_6 at geometries of neutral and ionized system using RKS/B3LYP+D3/aug-cc-pVTZ for RHF-SCF, RMP2, and RKS methods.

System	**C_6Cl_6**		**$C_6Cl_6^+$**		**$C_6Cl_6^-$**	
Geometry	neutral	anion	neutral	cation	neutral	anion
RHF-SCF	-2984.346506	-2984.263442	-2984.018226	-2984.027835	-2984.304053	-2984.344016
RMP2	-2986.464580	-2986.388667	-2986.117420	-2986.126892	-2986.464917	-2986.482805
RKS. B3LYP	-2989.562438	-2989.497801	-2989.231727	-2989.237619	-2989.576324	-2989.597158
RKS, B3LYP+D3	-2989.566924	-2989.502321	-2989.236213	-2989.242182	-2989.580810	-2989.601678

References

1 A. Schäfer, C. Huber and R. Ahlrichs, Fully optimized contracted Gaussian basis sets of triple zeta valence quality for atoms Li to Kr, *J. Chem. Phys.*, 1994, **100**, 5829–5835.

2 F. Neese, The ORCA program system, *Wiley Interdiscip. Rev. Comput. Mol. Sci.*, 2012, **2**, 73–78.

3 H.-J. Werner, P. J. Knowles, G. Knizia, F. R. Manby and M. Schütz, Molpro: A general-purpose quantum chemistry program package, *Wiley Interdiscip. Rev. Comput. Mol. Sci.*, 2012, **2**, 242–253.

4 S. Grimme, J. Antony, S. Ehrlich and H. Krieg, A consistent and accurate ab initio parametrization of density functional dispersion correction (DFT-D) for the 94 elements H-Pu, *J. Chem. Phys.*, 2010, **132**, 154104.

5 B. Ruščić, L. Klasinc, A. Wolf and J. V. Knop, Photoelectron spectra of and ab initio calculations on chlorobenzenes. 3. Hexachlorobenzene, *J. Phys. Chem.*, 1981, **85**, 1495–1497.

6 W. B. Knighton, J. A. Bognar and E. P. Grimsrud, Reactions of Selected Molecular Anions with Oxygen, *J. Mass Spectrom.*, 1995, **30**, 557–562.

7 J. R. Wiley, E. C. M. Chen, E. S. D. Chen, P. Richardson, W. R. Reed and W. E. Wentworth, The determination of absolute electron affinities of chlorobenzenes, chloronaphthalenes and chlorinated biphenyls from reduction potentials, *J. Electroanal. Chem.*, 1991, **307**, 169–182.